Journal of Photochemistry & Photobiology A: Chemistry 377 (2019) 67–74

Contents lists available at ScienceDirect

Journal of Photochemistry & Photobiology A: Chemistry

journal homepage: www.elsevier.com/locate/jphotochem

The role of distance between donor and acceptor in configuration stability of *Z/E* isomers based on cyanostilbene

Chendong Xu[a], Yujie Dong[a,*], Weijun Li[a], Ruiyang Zhao[b], Yuyu Dai[a], Cheng Zhang[a,*,1], Qingbao Song[a,*]

[a] State Key Laboratory Breeding Base of Green Chemistry Synthesis Technology, College of Chemical Engineering, Zhejiang University of Technology, Hangzhou 310014, PR China

[b] College of Chemical Engineering, Qingdao University of Science and Technology, Qingdao, 266042, PR China

ARTICLE INFO

Keywords:
Organic photo-electronic
D-A structure
Stable *Z/E* structure
Cyanostilbene
AIE

ABSTRACT

Cyanostilbene has been widely used in the design of photoelectrical materials, and our previous work has confirmed its *Z/E* isomerization reaction under photoirradiation can be suppressed by forming a suitable donor-acceptor (D-A) structure. In this work, we report two D-A cyanostilbene derivatives with AIE activity, abbreviated as PZPNC and PZNC, whose chemical structures only differ by one more phenyl between donor and acceptor. Their *Z/E* isomers were characterized with single crystal structures and the impact of D-A distance on their stability of *Z/E* configuration was studied. The in-situ UV–vis spectra and HPLC results of *Z/E*-PZPNC and *Z/E*-PZNC under photoirradiation demonstrated that the *Z/E* isomerization reaction of PZNC was slower than PZPNC, indicating that the shorter D-A distance is conductive to the stability of cyanostilbene due to the relatively stronger charge transfer state with lower energy.

1. Introduction

As a significant role in organic photoelectric functional materials, cyanostilbene (CNS) has attracted more and more attention to construct fluorescent molecules especially since that reported by Park etc. [1]. Various organic fluorescent molecules based on CNS have been reported and extensively exploited in nanomaterials [2–4], organic lasers [5,6], cell imaging [7–9], sensors [10–12], organic light-emitting diodes (OLEDs) [13,14], security ink [15], optical switching [16], luminous multifunctional materials [17,18] and so on. However, the different impact on luminescenc;1;e from *Z*- and *E*- configuration was scarcely reported, although the isomerization reaction under photo irradiation is so common for the most of fluorescent materials based on CNS. Definitely, to design and obtain this kind of molecules with stable *Z/E* configuration is beneficial to their practical applications.

Recently, we reported the *Z*- and *E*- isomers of two pairs of donor-acceptor (D-A) molecules (TPNCF and PZNCF) with CNS as acceptor, and triphenylamine [19] and phenoxazine [20] as donor respectively. The spectroscopy investigation indicated that both of TPNCF and PZNCF could keep their stable *Z/E* configuration in high polar solvents under photo irradiation. These work demonstrated that stable *Z/E* configuration under photo irradiation can be obtained through constructing a reasonable D-A structure, in which the *Z/E* isomerization reaction at the higher-energy located excited (LE) state is suppressed by the rapid internal conversion process from LE to the lower-energy charge transfer (CT) state [19–21].

In order to further investigate the relationship between molecular structure and configuration stability, herein, we report two pairs of D-A type *Z/E* isomers of PZPNC and PZNC based on phenoxazine and CNS, whose chemical structures only differ by one more phenyl between phenoxazine and CNS. The pure four compounds of *Z*-PZPNC, *E*-PZPNC, *Z*-PZNC and *E*-PZNC as well as their crystal structures were obtained. The photophysical properties and density functional theory (DFT) calculation suggested the formation of CT state in their excited state. In-situ UV–vis absorption spectra and high performance liquid chromatography (HPLC) demonstrated that the *Z/E* isomerization reaction rate in the case of *Z*-PZNC and *E*-PZNC became slower than that of *Z*-PZPNC and *E*-PZPNC under photo irradiation, i.e., the shorter distance between phenoxazine and CNS induced a more stable *Z/E* configuration in excited state. The results provide a strong evidence for the truth that *Z/E* isomerization reaction of CNS can be effectively restrained at excited state by modifying the D-A distance. It paves the way for further rational design of organic luminescent molecules containing double bond units.

* Corresponding authors.
E-mail addresses: dongyujie@zjut.edu.cn (Y. Dong), czhang@zjut.edu.cn (C. Zhang), qbsong@zjut.edu.cn (Q. Song).
[1] Homepage: http://www.czhang.zjut.edu.cn/chinese/index.htm.

https://doi.org/10.1016/j.jphotochem.2019.03.035
Received 17 January 2019; Received in revised form 9 March 2019
Available online 25 March 2019

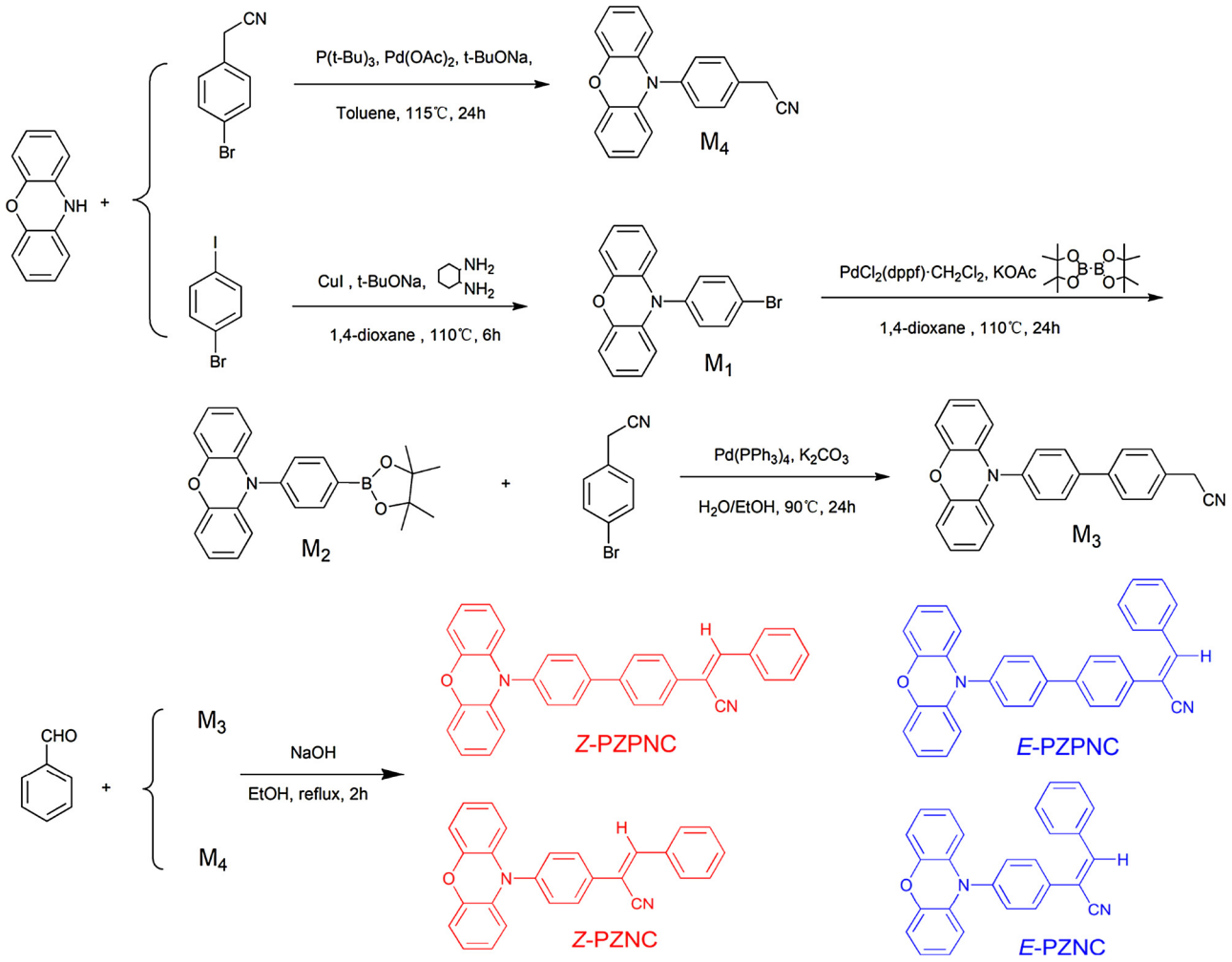

Scheme 1. The scheme of synthesis route and molecule structures of *Z*/*E*-PZPNC and *Z*/*E*-PZNC.

2. Results and discussion

2.1. Design and synthesis

To add a phenyl between phenoxazine and CNS group, we synthesized M_3 by two-step Suzuki coupling reaction [22]. The *Z*/*E*-PZPNC and *Z*/*E*-PZNC were prepared via the Knoevenagel reaction of phenoxazine-substituted benzyl cyanide (M_3 and M_4) and benzaldehyde, as shown in Scheme. 1 [23,24]. The *Z*/*E* isomers can be obtained directly by column chromatography. All compounds were fully characterized by NMR spectral analysis, MS spectroscopy and X-ray crystallography.

2.2. Crystal structure

By slow diffusion of methanol vapour into chloroform solution, we successfully obtained single crystal of *Z*/*E*-PZNC and *Z*/*E*-PZPNC suited for X-ray structural analysis. All the crystals are of yellow emissions under UV light. The single crystal structures clearly demonstrated the corresponding *Z* and *E* configurations of the four molecules. As shown in Fig. 1, *Z*-PZPNC and *Z*-PZNC show an almost planar stilbene structure with phenyl groups at the double bond ends forming a conjugated plane, while *E*-PZPNC and *E*-PZNC show a relatively twisted configuration at the stilbene part. All four molecules have a large twist angle (67–86°) between the nearly planar phenoxazine and the adjacent phenyl, which effectively break the conjugation between the donor of phenoxazine and acceptor of cyanostilbene, and are beneficial to the generation of charge transfer transition. On the other hand, the *Z* and *E* configurations also impact the packing modes of the two pairs of isomers in their crystals. For their *Z*-type crystals, the adjacent molecules pack to form weak π–π interactions between the less overlapped phenoxazine units (*Z*-PZPNC) and stilbene part (*Z*-PZNC). It is obvious that no coaxial π–π interactions in their *E*-type crystals due to the large intermolecular distance. Generally, all these molecules in their crystals display highly twisted configuration, which prevents the forming of strong π–π interactions and ensures the higher-efficiency fluorescence emission in crystal.

2.3. Photophysical properties

The UV–vis and PL spectra of *Z*/*E*-PZPNC and *Z*/*E*-PZNC were measured in toluene. As shown in Fig. 2a, there are two obvious absorption bands with λ_{max} around 318 nm and 309 nm at short wavelength and 414 and 401 nm at long wavelength in *Z*-PZNC and *E*-PZNC. Compared with PZNC, PZPNC molecules exhibit a continuous broad absorption band, which is actually contributed by two main absorption bands with λ_{max} around 329 nm and 400 nm for *Z*-PZPNC and 314 nm and 388 nm for *E*-PZPNC. Considering the nearly no conjugation between phenoxazine and cyanostilbene, the absorption at long wavelength should be attributed to the generation of lower-energy charge transfer transition. Thus, in comparison with PZPNC, the relatively red shifted absorption bands at long wavelength in PZNC suggest there is a stronger CT state in PZNC molecules. This also can be observed in the normalized PL spectra (Fig. 2b) of these four molecules, in which *Z*-PZNC (λ_{max} = 571 nm) and *E*-PZNC (λ_{max} = 587 nm) displayed

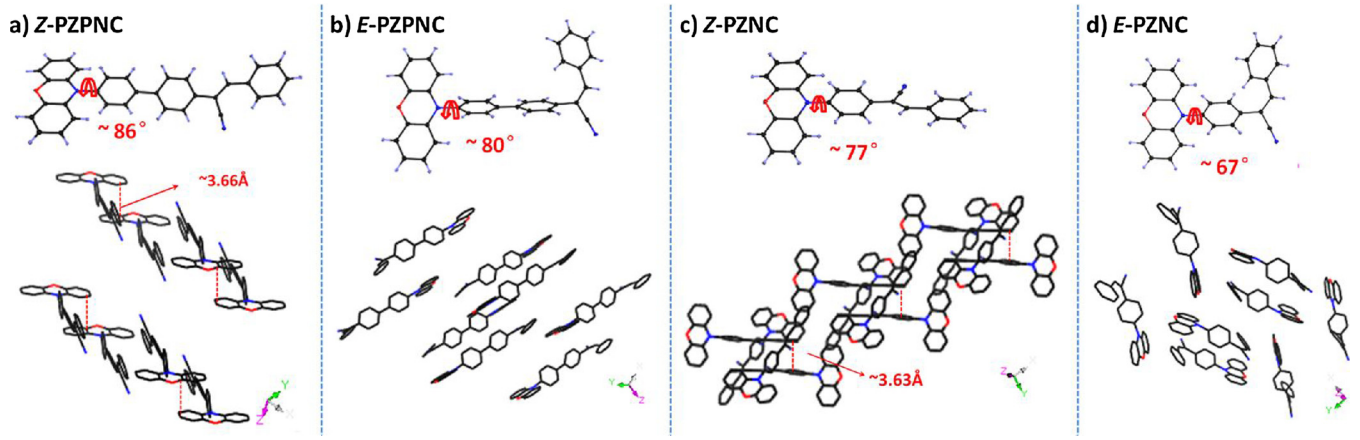

Fig. 1. the single crystal structures and packing diagrams of *Z*/*E*-PZPNC and *Z*/*E*-PZNC molecules.

obvious redshifts of ~50 nm in comparison with *Z*-PZPNC (λ_{max} = 529 nm) and *E*-PZPNC (λ_{max} = 535 nm) under the same conditions.

The solvent effect of the four compounds was also studied to further investigate their excited state properties. As shown in Fig. 3, all the four compounds displayed strong emission in non-polar solvent of hexane. Upon increasing the solvent polarity, the emission decreased obviously in intensity and even plummeted to nearly invisible in ethyl acetate. Meanwhile, obvious red-shifts can be observed with increasing the solvent polarity for all molecules, indicating again there is a CT state in their excited state of the four compounds.

Due to the lower-energy CT state, all these compounds show weak emission in dilute solutions. However, the stronger luminescence in their film demonstrates that they are aggregation-induced emission (AIE) active molecules, which are weak or non-luminescent in solution but show stronger luminescence in aggregate state [25]. This can be easily verified by testing the PL spectra in mixed solvent with the decreasing of solubility. As shown in Fig. 4, in an acetonitrile/water (ACN/H_2O) mixture system, all compounds are nonluminous in pure acetonitrile solution and the PL spectra did not show any obvious changes below 60% of water content. Upon further increasing the water fraction, the PL intensity was gradually increased, indicating their aggregates were formed in the solution mixtures with higher ratio of water and the fluorescent emission was boosted at the same time.

2.4. DFT analysis

To confirm the charge transfer excited state properties of the four compounds, theoretical calculation of electronic orbital distribution and energy level were carried out by B3LYP method. As shown in Fig. 5, DFT analysis demonstrated that the highest occupied molecular orbitals (HOMO) of all the four compounds were mainly located at the phenoxazine part, while their lowest unoccupied molecular orbitals (LUMO) were completely distributed at cyanostilbene group. The totally separate HOMO and LUMO distribution indicated the charge transfer character in the excited state for both *Z*/*E*-PZNC and *Z*/*E*-PZPNC. There were no obvious differences in the electron cloud distributions and electron transition characters between *Z*/*E*-PZNC and *Z*/*E*-PZPNC molecular cases. The calculated energy levels of HOMO are −4.66 eV (*Z*-PZPNC), −4.68 eV (*E*-PZPNC), −4.70 eV (*Z*-PZNC), and −4.74 eV (*E*-PZNC). Meanwhile, the LUMOs are calculated to be −2.26 eV (*Z*-PZPNC), −2.16 eV (*E*-PZPNC), −2.30 eV (*Z*-PZNC) and −2.19 eV (*E*-PZNC). These similar separated electron cloud distribution and close energy level results of electronic orbitals demonstrate the similar strong charge transfer transition character in the four molecules.

2.5. Electrochemistry

The electrochemical properties of PZPNC and PZNC were investigated to evaluate their electronic energy levels [26–28]. As shown

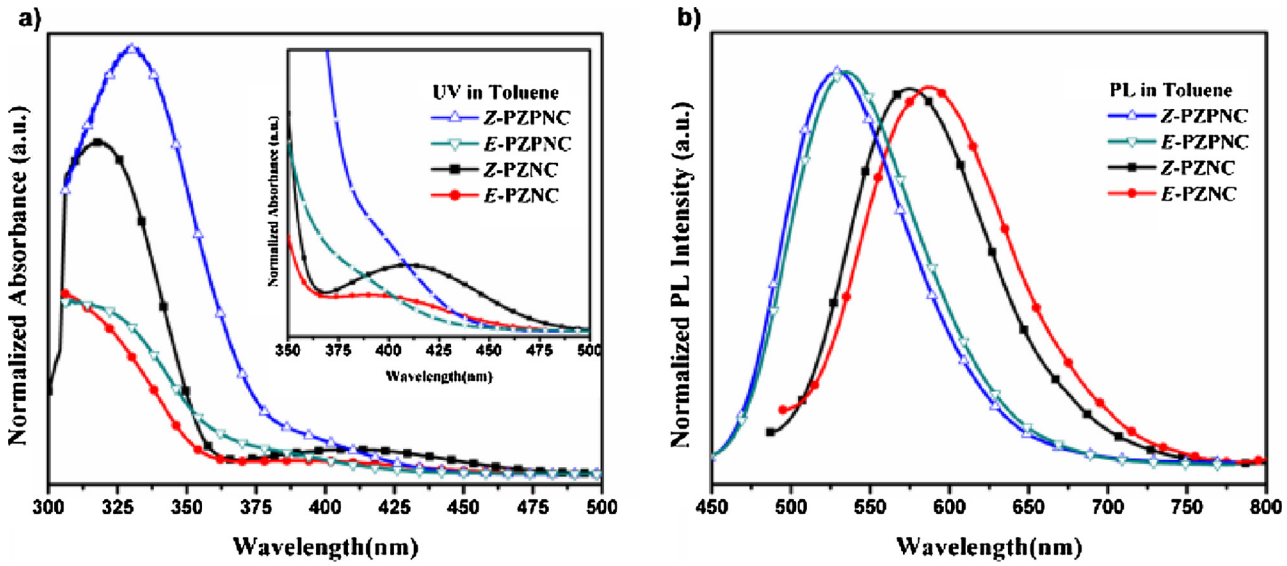

Fig. 2. The UV–vis and PL spectra of *Z*/*E*-PZPNC and *Z*/*E*-PZNC in toluene at 10^{-5} M.

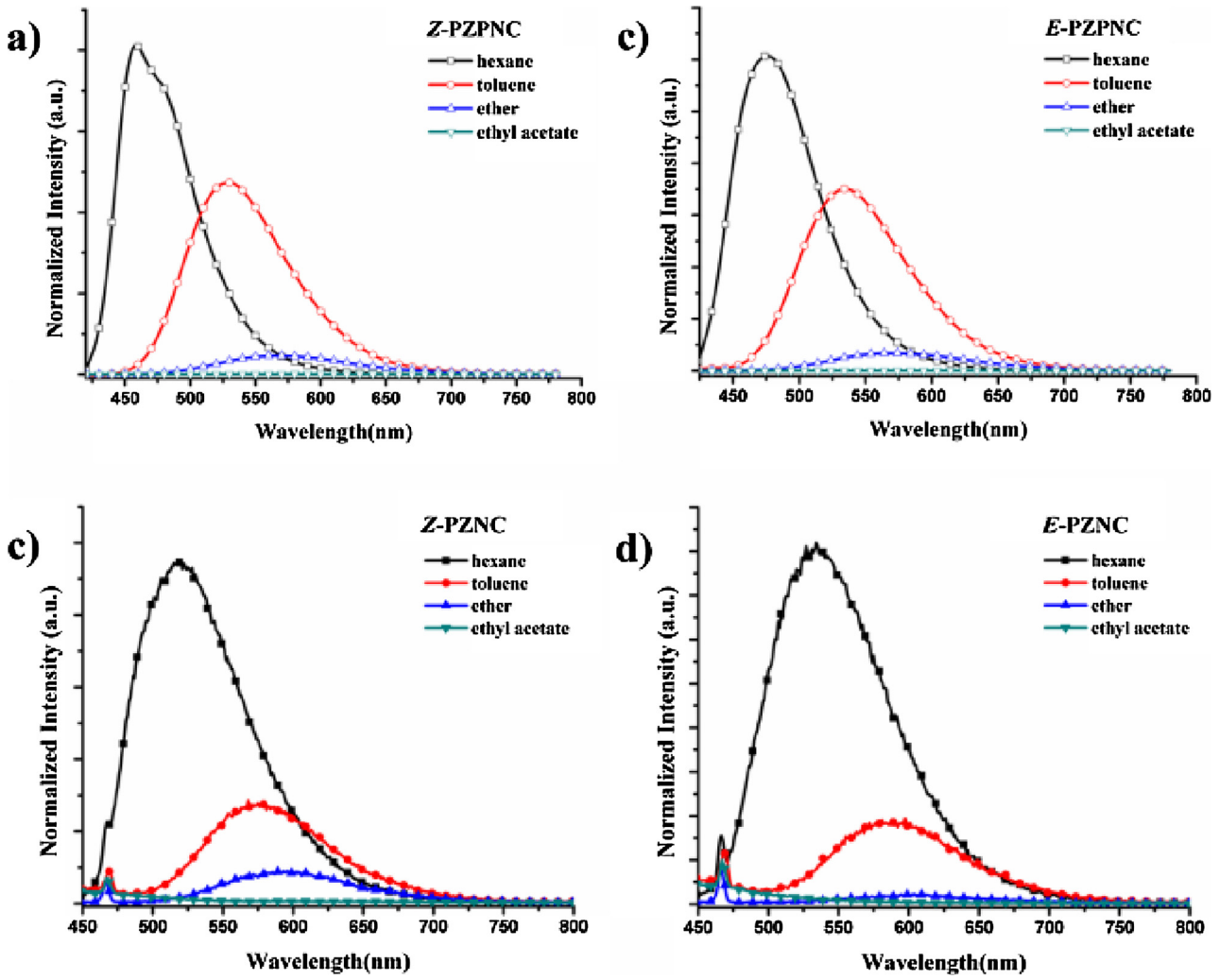

Fig. 3. The PL spectra of *Z*/*E*-PZPNC and *Z*/*E*-PZNC molecules in different solvents.

in Table 1, *Z*-PZPNC and *E*-PZPNC exhibited similar onset oxidative potential (0.70 V and 0.71 V) and the two isomers of PZNC also showed similar onset oxidative potential (0.74 V and 0.75 V). The HOMOs were calculated by the cyclic voltammetry method with *Z*-PZPNC and *E*-PZPNC (−5.10 eV, −5.11 eV) a little higher than *Z*-PZNC and *E*- PZNC (−5.14 and −5.15 eV), which is consistent with the results of theoretically calculation. The LUMOs of *Z*/*E*-PZPNC (−2.34/−2.29 eV) and *Z*/*E*-PZNC (−2.59/−2.54 eV) were calculated from the energy gap (E_g), which is estimated from the onset energy of the absorption curve (see Fig. 2). Obviously, the LUMOs of PZNC is lower than those of PZPNC, and charge transfer can easier happened in PZNC than PZPNC [29].

2.6. *Z*/*E* configuration stability

As a strong electron donating group, phenoxazine has exhibited the ability to stabilize the *Z*/*E* configurations of cyanostilbene in our previous work [19–21]. A distinct characteristic of this kind of D-A type molecules is that the isomerization reactions become slow as the increasing of solvent polarity. This could be confirmed by the in-situ UV–vis spectra and in-situ NMR spectra in solvents with different polarity. As shown in Figs. S1 and S2, under UV-irradiation, the *Z* and *E* isomers display a fast isomerization process with their absorption curves shift toward each other in the low-polar solvents (hexane, toluene and ether). However, when measured in the moderate-polar solvent of ethyl acetate, their isomerization reaction became very slow in rate without reaching the equilibrium in 30 min. We also measured their ^{1}H NMR spectra in non-polar deuterated toluene (Toluene-D8) and observed obvious chemical shift alteration between *Z* and *E* type for both of PZPNC and PZNC after 20 min photo irradiation (Fig. S3). These results are consistent with our previous conclusions, i.e., the stable *Z*/*E* configuration under photo irradiation is achievable by stabilizing CT state to be the lowest excited state.

In order to investigate the *Z*/*E* isomerization or configuration stability of PZPNC and PZNC, we further compared their in-situ UV–vis spectra in toluene. As shown in Fig. 6, both of *Z*/*E*-PZPNC and PZNC isomers started to move on the contrary under UV irradiation, indicating the happen of isomerization reaction. It is noticeable that the *Z*/*E* isomerization reaction of *E*-PZPNC happened quickly and reached the equilibrium in 2 min, but *Z*-PZPNC needed above 5 min to reach the equilibrium. However, for both of *Z*-PZNC and *E*-PZNC, their isomerisation process became obviously slower without reaching the equilibrium in 10 min under photo irradiation. The results indicate PZPNC molecules with a longer D-A distance are less stable than PZNC molecules in *Z*/*E* configuration.

To further demonstrate the result, the HPLC of these molecules pretreated with UV light (365 nm) in different irradiation time was performed and analysed. As shown in Fig. 7, the ratio of *Z*-PZNC, *E*-PZNC, *Z*-PZPNC and *E*-PZPNC decrease to 94%, 83%, 91% and 69% after 10 min irradiation, and were further reduced to 93%, 75%, 87% and 55% after 20 min irradiation. We could find that the *Z*/*E* isomerization reaction rate of *E*-type isomers was much faster than *Z*-type

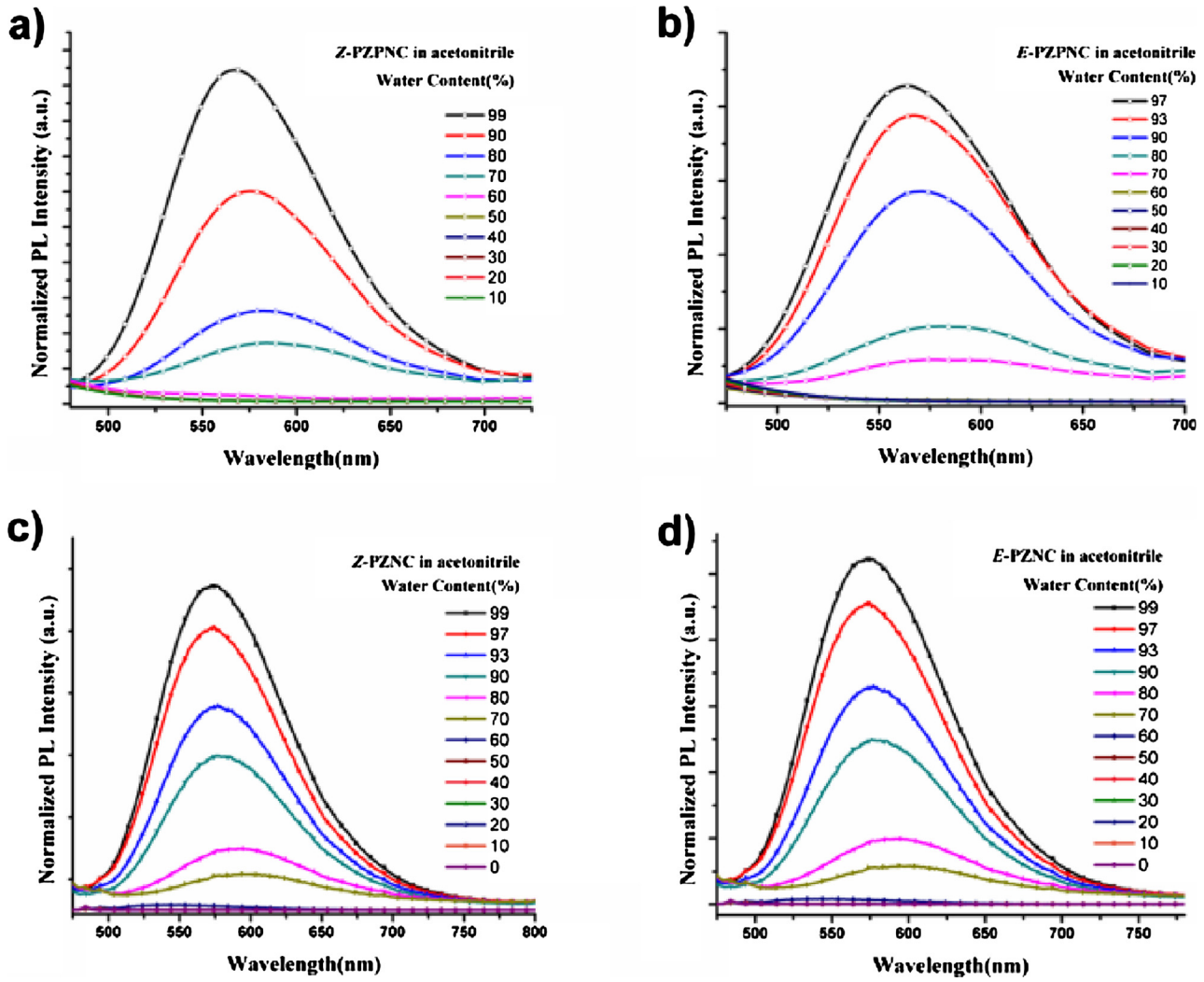

Fig. 4. PL spectra of PZPNC and PZNC in acetonitrile/water mixtures with different water fractions.

ones, and that of PZPNC was faster than PZNC. The analytical HPLC results agree to in-situ UV–vis spectra, and again confirm that the longer distance between donor and acceptor of CNS group is not conductive to the configuration stability of *Z/E* isomers.

3. Conclusions

We synthesized two pairs of D-A type *Z/E* isomers (PZPNC and PZNC) based on phenoxazine and cyanostilbene with different D-A distance between donor and acceptor, and studied their *Z/E* configuration stability. The spectroscopy investigation demonstrated a longer distance between donor and acceptor could not help to stabilize *Z/E* configuration. These results further confirmed our previous mentioned mechanism, that is the *Z/E* configuration, which is stable under photo irradiation, could be obtained by constructing a reasonable D-A structure. We believed this guideline could be further developed in other molecular structural design with double bond to achieve more configuration-stable molecules for organic photo-electronic applications.

4. Experimental section

4.1. General remarks

All the reagents or chemicals were commercial products without further purification. ^{1}H NMR spectra of the synthesized compounds were recorded on Bruker AVANCE III instrument (Bruker, Switzerland). Mass spectra (MALDI-TOF-MS) analysis was recorded using an AXIMA-CFRTM plus instrument and Mass spectra (ESI-MS) analysis was recorded using the ThermoFisher LCQTM Deca XP plus and Agilent 1200-6210 instrument. Photophysical properties were investigated by a Shimadzu UV-1800 spectrophotometer (Shimadzu, Japan) and a Perkin-Elmer LS-55 luminescence spectrophotometer (the integration time were set to be 0.01 s in order to shorten the measurement time to be less than 20 s). The photo irradiation was carried in a ZF-20D ultraviolet analyzer (YUHUA, China) with a UV light (365 nm, 24 W). High Performance Liquid Chromatography (HPLC) of the four isomers were recorded by the Agilent Technologies 1260 Infinity (Agilent, America). Electrochemical measurements were conducted by a CHI660E electrochemical analyser (Chenhua, China), with glassy carbon as the working electrode, platinum wire as the auxiliary electrode and Ag/Ag^{+} as the reference electrode, 0.1 mol L^{-1} tetrabutylammonium hexafluorophosphate (Bu_4NPF_6) dissolved in acetonitrile was employed as the supporting electrolyte.

4.2. Synthesis of 10-(4-bromophenyl)-10H-phenoxazine(M_1)

In a dry nitrogen atmosphere, a mixture of phenoxazine (0.92 g, 5 mmol), 1-bromo-4-iodobenzene (1.7 g, 6 mmol), sodium tert-butoxide (1.06 g, 11 mmol), cuprous iodide (0.02 g, 0.11 mmol) and 1, 2-diaminocyclohexane (0.07 g, 0.6 mmol) in 20 ml dry 1, 4-dioxane was heated

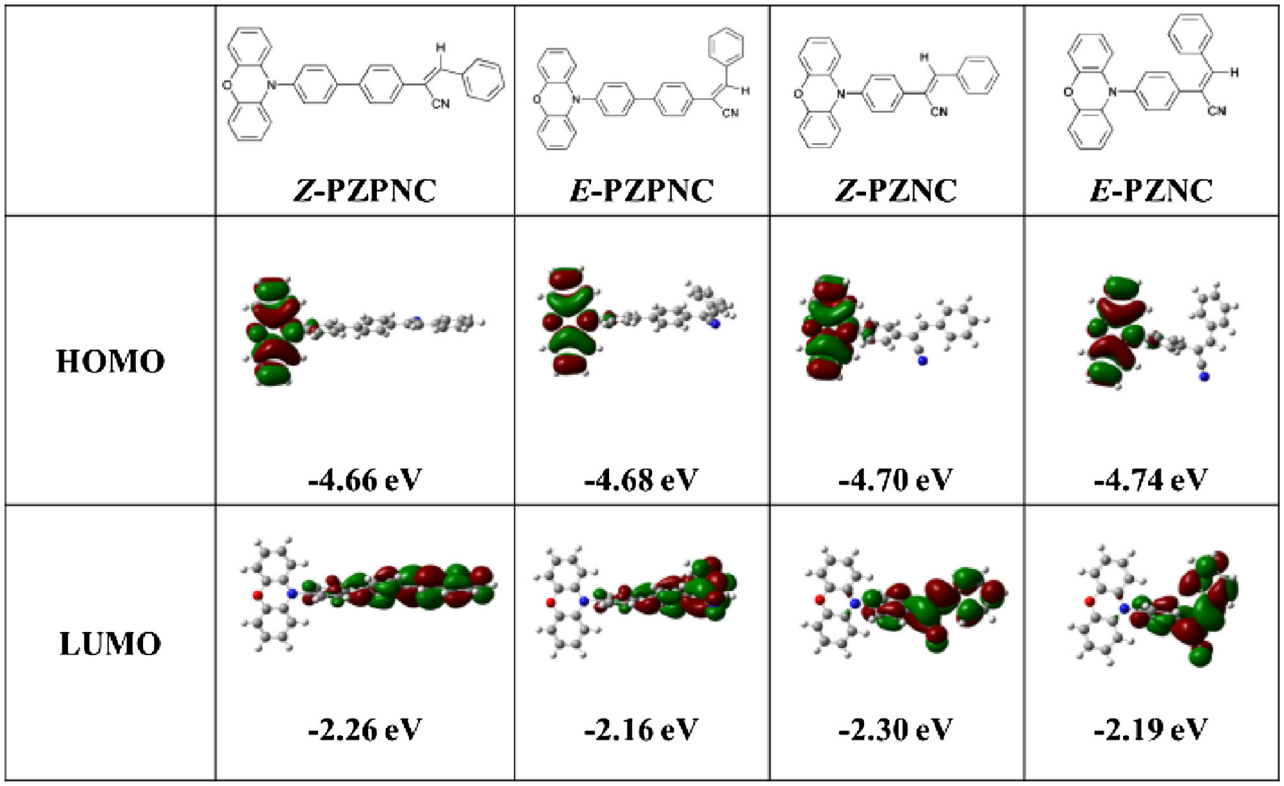

Fig. 5. The electron cloud distribution of electronic orbitals HOMO and LUMO for optimized *Z*/*E*-PZPNC and *Z*/*E*-PZNC molecules.

Table 1
Physical property of PZPNC and PZNC.

Compd.	E_{ox} [a] [V]	λ_{abs} [b] [nm]	E_{HOMO} [c] [eV]	E_{LUMO} [d] [eV]	E_g [e] [eV]	λ_{max} [f] [nm]
Z-PZPNC	0.70	450	−5.10	−2.34	2.76	529
E-PZPNC	0.71	440	−5.11	−2.29	2.82	535
Z-PZNC	0.74	487	−5.14	−2.59	2.55	571
E-PZNC	0.75	475	−5.15	−2.54	2.61	587

[a] E_{ox} = the onset oxidative potential.
[b] λ_{abs} = the onset value of the absorption peak.
[c] E_{HOMO} = highest occupied molecular orbitals calculated from the onset oxidative potential.
[d] E_{LUMO} = lowest unoccupied molecular orbitals estimated using E_{HOMO} and E_g.
[e] E_g = energy band gap calculated from the onset absorption spectrum.
[f] λ_{max} = the peak value of PL curve [23–25].

under 110 °C for 6 h. After the reaction, the mixture was cooled to room temperature and quenched with water and extracted with chloroform. The combined organic layer was washed with distilled water three times and dried over anhydrous magnesium sulfate. Then the solvent was evaporated in a vacuum. The crude product was purified by column chromatography on silica gel using petroleum ether/dichloromethane (9/1 v/v) as the eluent to obtain the product as white solid (1.13 g, 67%). ^{1}H NMR (500 MHz, $CDCl_3$) δ (TMS, ppm) 7.75 (d, *J* = 8.5 Hz, 2H), 7.26 (d, *J* = 8.5 Hz, 2H), 6.61–6.73 (m, 6H), 5.94 (d, *J* = 7.8 Hz, 2H). MS (ESI) (mass *m*/*z*): 338.3 $[M+H]^+$, $C_{18}H_{12}BrNO$ calc. 338.2.

4.3. Synthesis of 10-(4-(4, 4, 5, 5-tetramethyl-1, 3, 2-dioxaborolan-2-yl) phenyl)-10H-phenoxazine (M_2)

In a dry nitrogen atmosphere, a mixture of M_1 (0.2 g, 0.59 mmol), bis(pinacolato) diboron (0.19 g, 0.74 mmol), 1,1′-Bis(diphenylphosphino)ferrocene-palladiumdichloride dichloromethane adduct ($PdCl_2$(dppf)·CH_2Cl_2) (0.1 g, 0.13 mmol) and potassium acetate (0.6 g, 6.1 mmol) in 20 ml dry 1,4-dioxane was heated under 110 °C for 24 h. After the reaction, the mixture was cooled to room temperature and quenched with water and extracted with chloroform. The combined organic layer was washed with distilled water three times and dried over anhydrous magnesium sulfate. Then the solvent was evaporated in a vacuum. The crude product was purified by column chromatography on silica gel using petroleum ether/dichloromethane (2/1 v/v) as the eluent to obtain the product as white solid (0.12 g, 53%). ^{1}H NMR (500 MHz, $CDCl_3$) δ (TMS, ppm) 8.05 (d, *J* = 7.7 Hz, 2H), 7.37 (d, *J* = 7.9 Hz, 2H), 6.47–6.80 (m, 6H), 5.92 (d, *J* = 5.2 Hz, 2H), 1.4 (s, 12H). MS (ESI) (mass *m*/*z*): 386.2 $[M+H]^+$, $C_{24}H_{24}BrNO_3$ calc. 385.2.

4.4. Synthesis of 2-(4′-(10H-phenoxazin-10-yl)-[1, 1′-biphenyl]-4-yl) acetonitrile (M_3)

In a dry nitrogen atmosphere, a mixture of M_2 (0.51 g, 1.3 mmol), 4-bromophenylacetonitrile (0.38 g, 1.95 mmol), tetrakis(triphenylphosphine)palladium (0) (0.11 g, 0.10 mmol) and potassium carbonate (1.8 g, 13 mmol) in 25 ml H_2O/toluene (2/3 v/v) mixture solvent was heated under 90 °C for 24 h. After the reaction, the mixture was cooled to room temperature and quenched with water and extracted with chloroform. The combined organic layer was washed with distilled water three times and dried over anhydrous magnesium sulfate. Then the solvent was evaporated in a vacuum. The crude product was purified by column chromatography on silica gel using petroleum ether/dichloromethane (2/5 v/v) as the eluent to obtain the product as orange solid (0.30 g, 62%). ^{1}H NMR (500 MHz, $CDCl_3$) δ (TMS, ppm) 7.81 (d, *J* = 8.4 Hz, 2H), 7.69 (d, *J* = 8.3 Hz, 2H), 7.47 (d, *J* = 8.4 Hz, 2H), 7.44 (d, *J* = 8.4 Hz, 2H), 6.58–6.75 (m, 6H), 6.01 (d, *J* = 7.9 Hz, 2H), 3.85 (s, 2H, vinyl-H). MS (ESI) (mass *m*/*z*): 375.2 $[M+H]^+$ $C_{26}H_{18}N_2O$ calc. 374.3.

4.5. Synthesis of Z-PZPNC and E-PZPNC

To a mixture of M_3 (0.37 g, 1 mmol) and benzaldehyde (0.11 g,

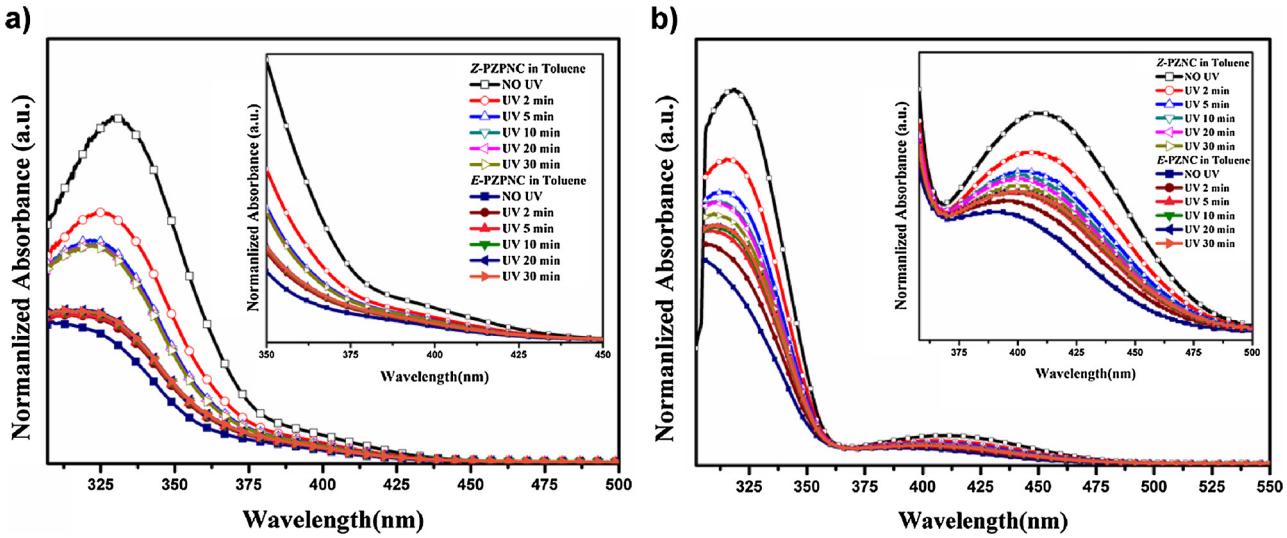

Fig. 6. The in-situ UV spectra of a) PZPNC and b) PZNC under different photo irradiated time of UV light (365 nm) in toluene.

1 mmol) in 10 ml ethanol, sodium hydroxide (0.04 g, 1 mmol) was added. The mixture was heated under 45 °C for 24 h, then cooled to room temperature and filtered. The residue was washed with cold ethanol by three times, and further purified by column chromatography via eluent (CH_2Cl_2/petroleum ether = 2/1) to obtain the products.

(*Z*)-2-(4′-Phenoxazin-10-yl-biphenyl-4-yl)-3-phenyl-acrylonitrile (*Z*-PZPNC). Yellow solid, 0.45 g, yield: 97%. ^{1}H NMR (500 MHz, $CDCl_3$) δ (TMS, ppm) 7.95 (d, J = 7.1 Hz, 2H), 7.86 (d, J = 8.4 Hz, 2H), 7.83 (d, J = 8.5 Hz, 2H), 7.76 (d, J = 8.6 Hz, 2H), 7.65 (s, 1H), 7.48–7.54 (m, 3H), 7.46 (d, J = 8.4 Hz, 2H), 6.72 (dd, J = 7.7 Hz, 1.7 Hz, 2H), 6.66 (dt, J = 15.2 Hz, 7.4 Hz, 4H), 6.03 (dd, J = 7.8 Hz, 1.6 Hz, 2H). MALDI-TOF MS (mass m/z): 463.8 $[M+H]^+$, $C_{33}H_{22}N_2O$ calc. 462.5.

(*E*)-2-(4′-Phenoxazin-10-yl-biphenyl-4-yl)-3-phenyl-acrylonitrile (*E*-PZPNC). Yellow solid, 0.01 g, yield: 3%. ^{1}H NMR (500 MHz, $CDCl_3$) δ

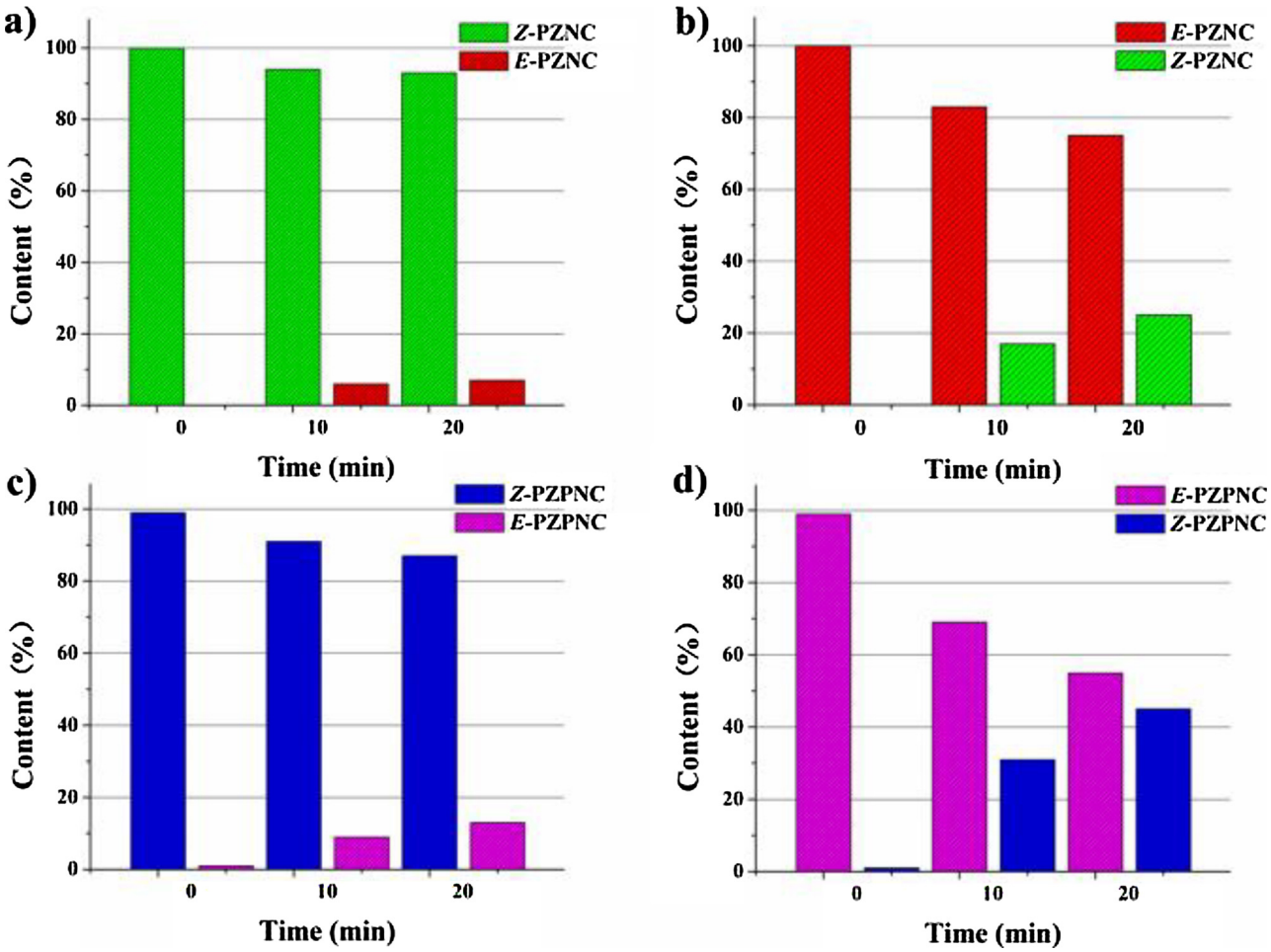

Fig. 7. The relative content of isomers recorded by HPLC (Samples were pretreated with 365 nm UV-irradiation for different time).

(TMS, ppm) 7.84 (d, J = 8.2 Hz, 2H), 7.67 (d, J = 8.3 Hz, 2H), 7.53 (d, J = 8.3 Hz, 2H), 7.41–7.84 (m, 3H), 7.28–7.36 (m, 3H), 7.26 (dd, J = 8.5 Hz, 1.5 Hz, 2H), 6.72 (d, J = 7.5 Hz, 2H), 6.61–6.66 (m, 4H), 6.00 (d, J = 7.0 Hz, 2H). MALDI-TOF MS (mass m/z): 463.8 $[M+H]^+$, $C_{33}H_{22}N_2O$ calc. 462.5.

4.6. Synthesis of 2-(4-(10H-phenoxazin-10-yl) phenyl) acetonitrile (M_4)

In a dry nitrogen atmosphere, a mixture of phenoxazine (0.37 g, 2 mmol), 4-bromophenylacetonitrile (0.47 g, 2.4 mmol), tri-*tert*-butylphosphine (0.11 g, 0.52 mmol), palladium acetate (0.03 g, 0.12 mmol) and sodium *tert*-butoxide (0.50 g, 5.2 mmol) in 30 ml toluene was heated under 115 °C for 24 h. After the reaction, the mixture was cooled to room temperature and quenched with water and extracted with chloroform. The combined organic layer was washed with distilled water three times and dried over anhydrous magnesium sulfate. Then the solvent was evaporated in a vacuum. The crude product was purified by column chromatography on silica gel using petroleum ether/dichloromethane (1/3, v/v) as the eluent to obtain the product as white solid (0.60 g, 50%). ^{1}H NMR (500 MHz, $CDCl_3$) δ (TMS, ppm) 7.59 (d, J = 8.4 Hz, 2H), 7.40 (d, J = 8.3 Hz, 2H), 6.56–6.75 (m, 6H), 5.90 (dd, J = 7.9 Hz, 1.4 Hz, 2H), 3.87 (s, 2H, alkyl-H). MS (ESI) (mass m/z): 297.1 $[M+H]^+$, $C_{28}H_{17}F_3N_2O$ calc. 298.3.

4.7. Synthesis of Z-PZNC and E-PZNC

To a mixture of M_4 (0.30 g, 1 mmol) and benzaldehyde (0.11 g, 1 mmol) in 10 ml ethanol, sodium hydroxide (0.04 g, 1 mmol) was added. The mixture was heated under 45 °C for 24 h, then cooled to room temperature and filtered. The residue was washed with cold ethanol by three times, and further purified by column chromatography via eluent (CH_2Cl_2/petroleum ether = 2/1) to obtain the products as yellow solid.

(*Z*)-2-(4-(10*H*-phenoxazin-10-yl)phenyl)-3-phenyl-acrylonitrile (*Z*-PZNC). Yellow solid, 0.33 g, yield: 87%. ^{1}H NMR (500 MHz, $CDCl_3$) δ (TMS, ppm) 7.90–7.99 (m, 4H), 7.64 (s, 1H), 7.49–7.56 (m, 3H), 7.47 (d, J = 8.5 Hz, 2H), 6.73 (dd, J = 8.5 Hz, 1.7 Hz, 2H), 6.66 (dt, J = 15.2 Hz, 7.3 Hz, 4H), 5.98 (dd, J = 7.9 Hz, 1.4 Hz, 2H). MALDI-TOF MS (mass m/z): 387.4 $[M+H]^+$, $C_{27}H_{18}N_2O$ calc. 386.4.

(*E*)-2-(4-(10*H*-phenoxazin-10-yl)phenyl)-3-phenyl-acrylonitrile (*E*-PZNC). Yellow solid, 0.02 g, yield: 5%. ^{1}H NMR (500 MHz, $CDCl_3$) δ (TMS, ppm) 7.62 (d, J = 8.4 Hz, 2H), 7.48 (s, 1H), 7.33–7.40(m, 3H), 7.30(t, J = 7.4 Hz, 2H), 7.24 (d, J = 7.3 Hz, 2H), 6.59–6.77 (m, 6H), 5.97 (d, J = 7.8 Hz, 2H). MALDI-TOF MS (mass m/z): 387.4 $[M+H]^+$, $C_{27}H_{18}N_2O$ calc. 386.4.

Conflicts of interest

There are no conflicts to declare

Acknowledgements

This study was supported by the Zhejiang Provincial Natural Science Foundation, China (LQ19E030016, LY19E030006, and LZ17E030001), the China Postdoctoral Science Foundation (2018M632498), the Zhejiang Provincial Postdoctoral Fellowship, China (Z71101009) and the National Natural Science Foundation of China (51603185, 51673174, 51703112 and 21875219).

Appendix A. Supplementary data

Supplementary material related to this article can be found, in the online version, at doi:https://doi.org/10.1016/j.jphotochem.2019.03.035.

References

[1] Byeong Kwan An, Deug Sang Lee, Jong Soon Lee, Yil Sung Park, Hyung Su Song, Soo Young Park, J. Am. Chem. Soc. 126 (2004) 10232–10233.
[2] Hyeong Ju Kim, Paramjyothi C. Nandajan, Johannes Gierschner, Soo Young Park, Adv. Funct. Mater. 28 (2018) 1705141–1705151.
[3] Xue Jin, Dong Yang, Yuqian Jiang, Pengfei Duan, Minghua Liu, Chem. Commun. 54 (2018) 4513–4516.
[4] Yanming Ren, Ruilin Zhang, Chao Yan, Tingyan Wang, Huifang Cheng, Xiaohong Cheng, Tetrahedron 73 (2017) 5253–5259.
[5] Byeong Kwan An, Johannes Gierschner, Soo Young Park, Acc. Chem. Res. 45 (4) (2012) 544–554.
[6] Yujie Dong, Suqian Ma, Xiaoyu Zhang, Jingyu Qian, Nianyong Zhu, Bin Xu, Cheuk Lam Ho, Wenjing Tian, Wai Yeung Wong, Sci. China Chem. 62 (2) (2019) 212–219.
[7] A. Gopinath, K. Ramamurthy, Mamangam Subaraja, Chellappan Selvaraju, A. Sultan Nasar, New J. Chem. 42 (2018) 10243–10253.
[8] Weijie Zhang, Chris Y.Y. Yu, Ryan T.K. Kwok, Jacky W.Y. Lam, Ben Zhong Tang, J. Mater. Chem. B 6 (2018) 1501–1507.
[9] Ka Young Kim, Hanyong Jin, Jaehyeon Park, Sung Ho Jung, Ji Ha Lee, Hyesong Park, Sung Kuk Kim, Jeehyeon Bae, Jong Hwa Jung, Nano Res. 11 (2) (2018) 1082–1098.
[10] Yao Ma, Massimo Cametti, Zoran Dz˝olic´, Shimei Jiang, J. Mater. Chem. C 6 (2018) 9232–9237.
[11] Yuyang Zhang, Jianyan Huang, Lin Kong, Yupeng Tian, Jiaxiang Yang, CrystEngComm 20 (2018) 1237–1244.
[12] Bin Wang, Chun Ying Wei, RSC Adv. 8 (2018) 22806–22812.
[13] Wenyan Fang, Wang Zhao, Pan Pei, Rui Liu, Yuyang Zhang, Lin Kong, Jiaxiang Yang, J. Mater. Chem. C 6 (2018) 9269–9276.
[14] Yujie Dong, Jingyu Qian, Yang Liu, Nianyong Zhu, Bin Xu, Cheuk Lam Ho, Wenjing Tian, Wai Yeung Wong, New J. Chem. 43 (2019) 1844–1850.
[15] Kenneth Yin Zhang, Xiaojiao Chen, Guanglan Sun, Taiwei Zhang, Shujuan Liu, Qiang Zhao, Wei Huang, Adv. Mater. 28 (2016) 7137–7142.
[16] Dojin Kim, Eon Kwon Ji, Soo Young Park, Adv. Funct. Mater. 28 (2018) 1706213–1706219.
[17] Marta Martínez-Abadía, Raquel Giménez, María Blanca Ros, Adv. Mater. 30 (2018) 1704161–1704199.
[18] Yujian Zhang, Moge Qile, Jingwei Sun, Minhong Xu, Kai Wang, Feng Cao, Weijun Li, Qingbao Song, Zou Bo, Cheng Zhang, J. Mater. Chem. C 4 (2016) 9954–9960.
[19] Weijun Li, Shizhao Wang, Yujian Zhang, Yujie Dong Yu Gao, Xiang Zhang, Qingbao Song, Bing Yang, Yuguang Ma, Cheng Zhang, J. Mater. Chem. C 5 (2017) 8097–8104.
[20] Yujie Dong, Chendong Xu, Shizhao Wang, Weijun Li, Qingbao Song, Cheng Zhang, Acta Phys. Chim. Sin. 35 (6) (2019) 637–643.
[21] Jin Liu, Weijun Li, Minjie Liu, Yujie Dong, Yuyu Dai, Qingbao Song, Jianli Wang, Cheng Zhang, Phys. Chem. Chem. Phys. 20 (2018) 28279–28286.
[22] InSeob Park, Sae Youn Lee, Chihaya Adachi, Takuma Yasuda, Adv. Funct. Mater. 26 (2016) 1813–1821.
[23] Chunbo Duan, Jing Li, Chunmiao Han, Dongxue Ding, He Yang, Ying Wei, Hui Xu, Chem. Mater. 28 (2016) 5667–5679.
[24] Regis Guillot, Andre Loupy, Abdelkrim Meddour, Michele Pelletd, Alain Petit, Tetrahedron 61 (2005) 10129–10137.
[25] Yuanjing Cai, Lili Du, Kerim Samedov, Xinggui Gu, Fei Qi, Herman H.Y. Sung, Brian O. Patrick, Zhiping Yan, Xiaofang Jiang, Haoke Zhang, Jacky W.Y. Lam, Ian D. Williams, David Lee Phillips, Anjun Qin, Ben Zhong Tang, Chem. Sci. 9 (2018) 4662–4670.
[26] Yuyu Dai, Weijun Li, Xingxing Qu, Jin Liu, Shuanma Yan, Mi Ouyang, Xiaojing Lv, Cheng Zhang, Electrochim. Acta 229 (2017) 271–280.
[27] Weijun Li, Lan Chen, Yuyu Pan, Shuanma Yan, Yuyu Dai, Jin Liu, Yue Yu, Xingxing Qu, Qingbao Song, Mi Ouyang, Cheng Zhang, J. Electrochem. Soc. 164 (4) (2017) E84–E89.
[28] Weijun Li, Yuyu Pan, Ran Xiao, Qiming Peng, Shitong Zhang, Dongge Ma, Feng Li, Fangzhong Shen, Yinghui Wang, Bing Yang, Yuguang Ma, Adv. Funct. Mater. 24 (2014) 1609–1614.
[29] Weijun Li, Liang Yao, Haichao Liu, Zhiming Wang, Shitong Zhang, Ran Xiao, Huanhuan Zhang, Ping Lu, Bing Yang, Yuguang Ma, J. Mater. Chem. C 2 (2014) 4733–4736.